EUROFUSION WP14ER-PR(16) 14896

N Horsten et al.

Comparison of fluid neutral models with a kinetic model for a simplified 2D detached ITER case

Preprint of Paper to be submitted for publication in
22nd International Conference on Plasma Surface Interactions
in Controlled Fusion Devices (22nd PSI)

This work has been carried out within the framework of the EUROfusion Consortium and has received funding from the Euratom research and training programme 2014-2018 under grant agreement No 633053. The views and opinions expressed herein do not necessarily reflect those of the European Commission.

Assessment of fluid neutral models for a detached ITER case

N. Horsten[a,*], W. Dekeyser[b], G. Samaey[c], M. Baelmans[a]

[a] *KU Leuven, Department of Mechanical Engineering, Celestijnenlaan 300A, 3001 Leuven, Belgium*
[b] *ITER Organization, Route de Vinon-sur-Verdon, CS 90 046, 13067 St-Paul-lez-Durance, France*
[c] *KU Leuven, Department of Computer Science, Celestijnenlaan 200A, 3001 Leuven, Belgium*

Abstract

We compare the plasma sources (particle, parallel momentum and ion energy) due to plasma-neutral interactions computed with different fluid neutral models with the sources from a Monte Carlo simulation of the kinetic neutral equation. This is done for a fixed background plasma, which is representative for an ITER detached case. We illustrate that the reaction data from the AMJUEL-HYDHEL databases can be incorporated in the fluid models. A pure pressure-diffusion equation gives already accurate results for the particle source, but it is inaccurate for the momentum and energy source. A parallel momentum equation has to be added to achieve predictions of the momentum and energy source within 30% of accuracy. Newly developed boundary conditions, based on the diffusion approximation for incident neutrals, show to be crucial for accurate results of the fluid models close to the divertor target. The slight overestimation of the momentum and energy sources can be further reduced by adding a separate neutral energy equation.

Keywords: plasma edge modeling, neutrals, fluid approximation

1. Introduction

Plasma edge codes are crucial for the design of the divertor, plasma-facing components, and pumping systems of future fusion reactors. Most often, they are based on a kinetic description for the neutral particle transport, which is solved with Monte Carlo (MC) codes such as, e.g., EIRENE [1]. However, the statistical noise hampers the convergence of the plasma boundary codes and the increased number of ion-neutral interactions in detached regimes leads to exacerbated run times. Moreover, these issues make gradient-based optimization calculations unfeasible thus far.

Therefore, there is a need for a (partially) deterministic description of the neutrals to reduce both noise and calculation time. Multiple macroscopic fluid neutral models have been developed over the last decades [2–6]. However, the fluid approach is only valid in high-collisional regions of the simulation domain, where MC simulations become tedious.

*Corresponding author
Email address: niels.horsten@kuleuven.be (N. Horsten)

Therefore, a so-called hybrid neutral model, where the fluid and kinetic descriptions are combined, can be the solution [7], but the efficiency of such hybrid methods crucially depends on the quality of the fluid models that are used.

In this paper, we compare fluid neutral models (solved in the entire domain) of different degrees of complexity to the results of an MC simulation of the kinetic equation. To mimic as much as possible the microscopic physics of the EIRENE code, we use the AMJUEL-HYDHEL databases [8, 9] for the microscopic cross-sections and rate coefficients. The conversion of the databases to a fluid description is already covered in Ref. [10] for a 1D case. Here, we generalize it for the 2D plasma edge. We use a simplified model to describe the reflection of the neutrals at the boundaries (no molecules and the fast reflected particles get a fixed fraction of the energy of the incident particles) and we extend the 1D diffusion approach from Ref. [11] to 2D for the treatment of the recycled or reflected neutrals in the fluid models. This recycling/reflection model can easily be adapted for more sophisticated models such as the TRIM code database [12].

The introduction of the advanced databases for cross-sections and rate coefficients and the inclusion of the recycling/reflection model in the boundary conditions is new compared to other fluid models from literature, where simplified expressions are used for the rate coefficients and artificial boundary conditions are imposed. An example of a classic boundary condition is the assumption that the parallel neutral velocity at the target plate is a (user-defined) fraction of the parallel ion velocity [3, 4]. However, this fraction strongly depends on the plasma state itself and there is no a priori knowledge of its value. In addition, the traditional models contain even more user-defined fitting parameters for, e.g., flux limiters [3, 6] to match the fluid and kinetic models. The fluid models from this paper do not introduce extra (user-defined) parameters compared to the kinetic model.

This paper is outlined as follows. In Section 2, the kinetic neutral model is described. The fluid neutral models are elaborated in Section 3. We pay special attention to the boundary conditions in Section 4. The newly developed boundary conditions are derived from the underlying kinetic description and are key to achieve successful results. We compare the fluid models with the results from an MC simulation in Section 5 for a detached ITER case. We show that the fluid models perform well in this high-collisional case.

2. Kinetic neutral model

The neutral velocity distribution $f_\mathrm{n}(\mathbf{v})$ satisfies the steady-state kinetic (Boltzmann) equation:

$$\mathbf{v}\cdot\nabla f_\mathrm{n}(\mathbf{v}) = \widetilde{f}_\mathrm{i}(\mathbf{v}) n_\mathrm{i} n_\mathrm{e} K_\mathrm{r} + n_\mathrm{i} \int \sigma_\mathrm{cx}(E_\mathrm{c}) ||\mathbf{v}-\mathbf{v}'|| \widetilde{f}_\mathrm{i}(\mathbf{v}) f_\mathrm{n}(\mathbf{v}')\mathrm{d}\mathbf{v}' - f_\mathrm{n}(\mathbf{v})(n_\mathrm{i} K_\mathrm{cx}(\mathbf{v}) + n_\mathrm{e} K_\mathrm{i}), \quad (1)$$

with $\mathbf{v}$ the particle velocity vector, $\nabla = \nabla_\mathbf{x}$ the gradient with respect to the position $\mathbf{x}$ and $\widetilde{f}_\mathrm{i}(\mathbf{v})$ the normalized ion distribution (drifting Maxwellian) such that $\int \widetilde{f}_\mathrm{i}(\mathbf{v})\mathrm{d}\mathbf{v} = 1$, where the integral is taken over the whole velocity space. The ion, electron and neutral density are respectively n_i, n_e and $n_\mathrm{n} = \int f_\mathrm{n}(\mathbf{v})\mathrm{d}\mathbf{v}$.

Three processes are taken into account: volumetric (radiative and three-body) recombination, electron impact ionization and charge-exchange (CX) collisions with respectively rate coefficients K_r, K_i and K_cx. Because of the large thermal velocity of the electrons compared to the ions and the neutrals, the recombination and ionization rate coefficients are independent of the particle velocity and determined by polynomial fits with respect to the electron density and temperature in the AMJUEL database (reaction 2.1.8 for recombination and 2.1.5 for ionization [9]). The treatment of the CX collisions becomes more complicated due to the almost equal thermal velocities of the two colliding species. The second term on the right hand side of Eq. (1) corresponds to the source and $-f_\mathrm{n}(\mathbf{v})n_\mathrm{i}K_\mathrm{cx}(\mathbf{v})$ to the sink of neutrals due to CX collisions, with $\sigma_\mathrm{cx}(E_\mathrm{c})$ the microscopic cross-section, which is a function of the center-of-mass kinetic energy of the collision partners $E_\mathrm{c} = \frac{m}{4}||\mathbf{v}-\mathbf{v}'||^2$, with m the particle mass. The expressions for $\sigma_\mathrm{cx}(E_\mathrm{c})$ and $K_\mathrm{cx}(T_\mathrm{i}, E_\mathrm{n})$ are determined by reaction 3.1.8 of the AMJUEL-HYDHEL databases [8, 9], with T_i the ion temperature and E_n the kinetic energy of the neutral particle. There is an immediate relation between the microscopic cross-section and rate coefficient:

$$K_\mathrm{cx}(\mathbf{v}) = \int \sigma_\mathrm{cx}(E_\mathrm{c})||\mathbf{v}-\mathbf{v}'||\widetilde{f}_\mathrm{i}(\mathbf{v}')\mathrm{d}\mathbf{v}'. \tag{2}$$

It should be noted that all distribution functions, densities and temperatures depend on the spatial position.

3. Fluid neutral models

Taking moments of the Boltzmann equation (Eq. (1)) over velocity space leads to the neutral continuity, momentum and energy equations:

$$\nabla\cdot(n_\mathrm{n}\mathbf{V}_\mathrm{n}) = S_{n_\mathrm{n}}, \tag{3}$$

$$\nabla\cdot(mn_\mathrm{n}\mathbf{V}_\mathrm{n}\mathbf{V}_\mathrm{n}+\Pi_\mathrm{n}) = -\nabla p_\mathrm{n} + \mathbf{S}_{m\mathbf{V}_\mathrm{n}}, \tag{4}$$

$$\nabla\cdot\left(\left(\frac{5}{2}T_\mathrm{n} + m\frac{||\mathbf{V}_\mathrm{n}||^2}{2}\right)n_\mathrm{n}\mathbf{V}_\mathrm{n} + \Pi_\mathrm{n}\cdot\mathbf{V}_\mathrm{n} + \mathbf{q}_\mathrm{n}\right) = S_{E,\mathrm{n}}, \tag{5}$$

with $\mathbf{V}_\mathrm{n} = \frac{1}{n_\mathrm{n}}\int \mathbf{v}f_\mathrm{n}(\mathbf{v})\mathrm{d}\mathbf{v}$ the neutral drift velocity, $T_\mathrm{n} = \frac{1}{n_\mathrm{n}}\frac{m}{3}\int||\mathbf{c}||^2 f_\mathrm{n}(\mathbf{v})\mathrm{d}\mathbf{v}$ the neutral temperature, with $\mathbf{c} = \mathbf{v}-\mathbf{V}_\mathrm{n}$ the deviation from the drift velocity, and $p_\mathrm{n} = n_\mathrm{n}T_\mathrm{n}$ the neutral pressure. Eqs. (3)-(5) are not a closed system of equations due to the presence of the stress tensor $\Pi_\mathrm{n} = m\int \mathbf{c}\mathbf{c}f_\mathrm{n}(\mathbf{v})\mathrm{d}\mathbf{v} - p_\mathrm{n}\mathbb{I}$ and the heat flux vector $\mathbf{q}_\mathrm{n} = \frac{m}{2}\int||\mathbf{c}||^2\mathbf{c}f_\mathrm{n}(\mathbf{v})\mathrm{d}\mathbf{v}$. Here, $\mathbb{I}$ is the identity tensor. For sufficiently small deviations of $f_\mathrm{n}(\mathbf{v})$ from the equilibrium (Maxwellian) distribution, the Chapman-Enskog method [13] can be used, giving

$$\Pi_\mathrm{n} = -\eta^\mathrm{n}\left(\nabla\mathbf{V}_\mathrm{n} + (\nabla\mathbf{V}_\mathrm{n})^T - \frac{2}{3}(\nabla\cdot\mathbf{V}_\mathrm{n})\mathbb{I}\right), \tag{6}$$

$$\mathbf{q}_\mathrm{n} = -\kappa^\mathrm{n}\nabla T_\mathrm{n}, \tag{7}$$

with viscosity $\eta^\mathrm{n} = \frac{n_\mathrm{n}T_\mathrm{n}}{\nu_\mathrm{cx}}$ and heat conduction coefficient $\kappa^\mathrm{n} = \frac{5n_\mathrm{n}T_\mathrm{n}}{2m\nu_\mathrm{cx}}$. ν_cx the CX collision frequency.

The corresponding moments of the right hand side of Eq. (1) lead to the particle source S_{n_n}, momentum source $\mathbf{S}_{m\mathbf{V}_\mathrm{n}}$ and energy source $S_{E,\mathrm{n}}$ for the neutral fluid flow, given by

$$
\begin{aligned}
S_{n_\mathrm{n}} &= n_\mathrm{i} n_\mathrm{e} K_\mathrm{r} - n_\mathrm{n} n_\mathrm{e} K_\mathrm{i}, && (8)\\
\mathbf{S}_{m\mathbf{V}_\mathrm{n}} &= m n_\mathrm{i} n_\mathrm{e} K_\mathrm{r} \mathbf{V}_\mathrm{i} - m n_\mathrm{n} n_\mathrm{e} K_\mathrm{i} \mathbf{V}_\mathrm{n} + \mathbf{S}_{m\mathbf{V}_\mathrm{n},\mathrm{cx}}, && (9)\\
S_{E,\mathrm{n}} &= n_\mathrm{i} n_\mathrm{e} K_\mathrm{r} \left(\frac{3}{2} T_\mathrm{i} + \frac{m}{2} ||\mathbf{V}_\mathrm{i}||^2 \right) - n_\mathrm{n} n_\mathrm{e} K_\mathrm{i} \left(\frac{3}{2} T_\mathrm{n} + \frac{m}{2} ||\mathbf{V}_\mathrm{n}||^2 \right) + S_{E,\mathrm{n},\mathrm{cx}}, && (10)
\end{aligned}
$$

with $\mathbf{V}_\mathrm{i}$ the ion fluid velocity. The CX contributions ($\mathbf{S}_{m\mathbf{V}_\mathrm{n},\mathrm{cx}}$ and $S_{E,\mathrm{n},\mathrm{cx}}$) follow from

$$
\begin{aligned}
\left[\mathbf{S}^T_{m\mathbf{V}_\mathrm{n},\mathrm{cx}} \quad S_{E,\mathrm{n},\mathrm{cx}} \right]^T &= m n_\mathrm{i} \iint \left[\mathbf{v}^T \quad \tfrac{||\mathbf{v}||^2}{2} \right]^T \sigma_\mathrm{cx}(E_\mathrm{c}) ||\mathbf{v} - \mathbf{v}'|| \ldots \\
&\quad \ldots \left(\widetilde{f}_\mathrm{i}(\mathbf{v}) f_\mathrm{n}(\mathbf{v}') - \widetilde{f}_\mathrm{i}(\mathbf{v}') f_\mathrm{n}(\mathbf{v}) \right) \mathrm{d}\mathbf{v}\mathrm{d}\mathbf{v}'. \qquad (11)
\end{aligned}
$$

Eqs. (8)-(10) are the exact expressions of the source terms due to neutral-plasma interactions, at least if the real neutral velocity distribution is used in Eq. (11). However, for the fluid approach we always assume that the neutrals have a drifting Maxwellian distribution for the evaluation of the sources.

For many cases, this full Navier-Stokes model (Eqs. (3)-(5)) is computationally costly and therefore, there is a need for reduced models. In addition, the numerical evaluation of Eq. (11) is expensive and it is recommended to use alternative expressions. Three models with increasing degrees of complexity are considered in the next subsections.

3.1. Model 1: pressure-diffusion equation

The difficulties for solving the Navier-Stokes model especially originate from the nonlinear convective term in the momentum equation (Eq. (4)). However, if the transport is mainly driven by the pressure gradient, we can neglect the convective and viscous terms in Eq. (4). In addition, Fig. 1a shows that the momentum source due to CX collisions is approximately linear with the ion-neutral fluid velocity difference, at least if the velocity difference remains small compared to the thermal velocity and in case the neutral distribution is sufficiently close to a Maxwellian. The CX poloidal momentum source $S_{mu_{\mathrm{n}\theta},\mathrm{cx}}$ is shown, but the conclusions are the same for the other components (radial and toroidal). It can be seen that the drift velocity difference in the other directions has an influence on the slope of the line, especially for low temperatures. However, this influence is neglected by assuming that there is no ion-neutral fluid velocity difference in the other directions.

The slope of the line in the origin is the momentum linearized CX rate coefficient $K_{\mathrm{cx,m}}$, which is a function of the average of the ion and neutral temperatures (Fig. 1b). With this linearization, the CX momentum source can be approximated as

$$
\mathbf{S}_{m\mathbf{V}_\mathrm{n},\mathrm{cx}} \approx m n_\mathrm{n} n_\mathrm{i} K_{\mathrm{cx,m}} (\mathbf{V}_\mathrm{i} - \mathbf{V}_\mathrm{n}). \qquad (12)
$$

Neglecting the convective and viscous terms and linearizing the momentum source leads immediately to an expression for the particle flux density $n_\mathrm{n}\mathbf{V}_\mathrm{n}$, which can be imposed in

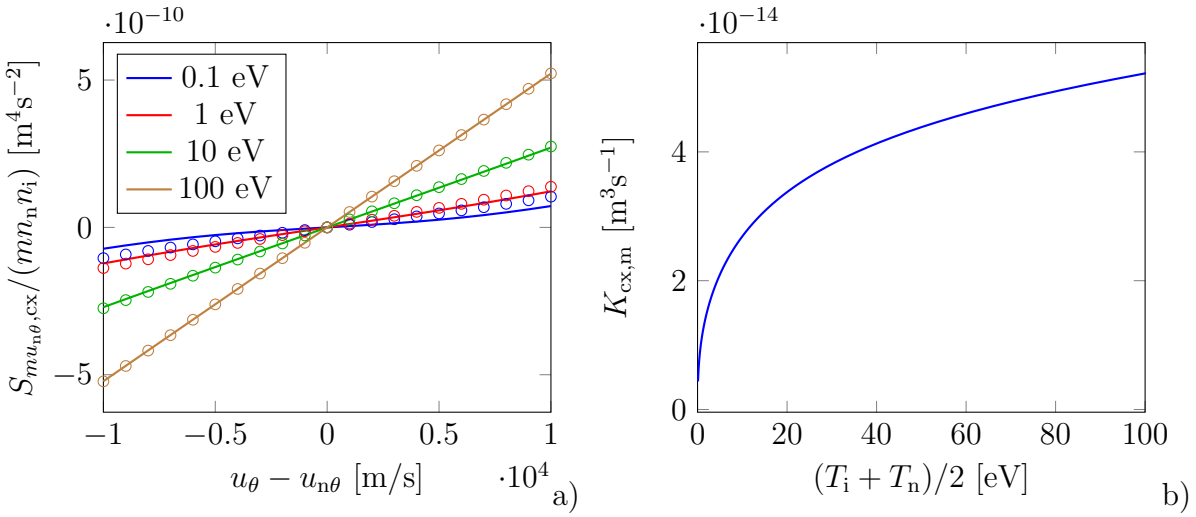

Figure 1: Determination of the momentum linearized CX rate coefficient. a) Poloidal CX momentum source divided by $mn_{\mathrm{n}}n_{\mathrm{i}}$ as a function of the poloidal ion-neutral velocity difference for different averages of the ion and neutral temperatures (solid lines for cases without drift velocity difference in radial and toroidal directions; circular marks for a velocity difference of $1 \cdot 10^4$ m/s in radial and toroidal directions. b) Momentum linearized CX rate coefficient.

the continuity equation (Eq. (3)). This combined continuity and momentum equation is called the pressure-diffusion equation:

$$\nabla \cdot \left(n_{\mathrm{n,eq}} \mathbf{V}_{\mathrm{i}} - D_p^{\mathrm{n}} \nabla p_{\mathrm{n}} \right) = S_{n_{\mathrm{n}}}, \tag{13}$$

with $n_{\mathrm{n,eq}} = (n_{\mathrm{i}} n_{\mathrm{e}} K_{\mathrm{r}} + n_{\mathrm{n}} n_{\mathrm{i}} K_{\mathrm{cx,m}})/(n_{\mathrm{i}} K_{\mathrm{cx,m}} + n_{\mathrm{e}} K_{\mathrm{i}})$ and $D_p^{\mathrm{n}} = (m\,(n_{\mathrm{i}} K_{\mathrm{cx,m}} + n_{\mathrm{e}} K_{\mathrm{i}}))^{-1}$. The first model consists of this single convection-diffusion equation, which is solved for the neutral pressure. In addition, it is assumed that the neutrals are in thermal equilibrium with the ions ($T_{\mathrm{n}} = T_{\mathrm{i}}$).

3.2. Model 2: pressure-diffusion and parallel momentum equation

The dominant ion-neutral friction parallel to the magnetic field requires accurate results for the parallel neutral velocity. Due to the fact that a fraction of the neutrals is emitted isotropically at the target, the magnitude of the parallel neutral velocity close to the target is lower than the ion parallel velocity. Therefore, for the second model a momentum equation parallel to the magnetic field is added. Thus, this model consists of the parallel component of Eq. (4) and the continuity equation (Eq. (3)), where the pressure-diffusion approximation is used for the transport in radial and diamagnetic directions. These equations are solved for the neutral density and neutral parallel velocity again assuming that $T_{\mathrm{n}} = T_{\mathrm{i}}$.

To easily derive the CX collision frequency ν_{cx}, which is needed to determine the viscosity η^{n}, the Boltzmann equation is approximated as

$$\mathbf{v} \cdot \nabla f_{\mathrm{n}}(\mathbf{v}) \approx \widetilde{f}_{\mathrm{i}}(\mathbf{v}) n_{\mathrm{i}} n_{\mathrm{e}} K_{\mathrm{r}} - f_{\mathrm{n}}(\mathbf{v}) n_{\mathrm{e}} K_{\mathrm{i}} + (\widetilde{f}_{\mathrm{i}}(\mathbf{v}) n_{\mathrm{n}} - f_{\mathrm{n}}(\mathbf{v})) n_{\mathrm{i}} K_{\mathrm{cx,m}}, \tag{14}$$

making use of the momentum linearized CX rate coefficient. This expression is verified in Section 5.3. This way, the CX collision frequency can be approximated as $\nu_{\mathrm{cx}} \approx n_{\mathrm{i}} K_{\mathrm{cx,m}}$.

3.3. Model 3: Pressure-diffusion, parallel momentum and energy equation

To take into account possible neutral-ion temperature differences, we add the energy equation (Eq. (5)) for model 3. Thus, model 3 is an extension of model 2 where it is no longer assumed that the ions and neutrals are in thermal equilibrium ($T_\mathrm{n} \neq T_\mathrm{i}$). Again, we use Eq. (14) to simplify the CX energy source from Eq. (11). This leads to

$$S_{E,\mathrm{n,cx}} = n_\mathrm{n} n_\mathrm{i} K_\mathrm{cx,m} \left(\frac{3}{2}(T_\mathrm{i} - T_\mathrm{n}) + \frac{m}{2}\left(||\mathbf{V}_\mathrm{i}||^2 - ||\mathbf{V}_\mathrm{n}||^2 \right) \right). \tag{15}$$

4. Treatment from the boundary conditions

The boundary conditions are of crucial importance to get accurate results for the fluid models. In literature it is most often assumed that the neutral parallel velocity at the target is a fraction of the ion parallel velocity [3, 4]. However, this fraction is a user-defined fitting parameter, which is case dependent.

In this paper, we use physics based boundary conditions, which do not need any user-defined fitting parameters. Particle, momentum and energy fluxes are imposed at all boundaries (at least if the fluid model contains the corresponding moment equation). These boundary fluxes correspond to the moments of the total neutral distribution at a particular position at a boundary $f_\mathrm{n,b}(\mathbf{v})$, which can be written as

$$f_\mathrm{n,b}(\mathbf{v}) = \begin{cases} f_{\mathrm{n},\nu-,\mathrm{b}}(\mathbf{v}) & \text{if} \quad \mathbf{v}\cdot\boldsymbol{\nu} \leq 0, \\ \int_{\mathbf{v}'\cdot\boldsymbol{\nu}\leq 0} (R^\mathrm{i}_\mathrm{b}(\mathbf{v}' \to \mathbf{v}) f_{\mathrm{i},\nu-,\mathrm{b}}(\mathbf{v}') + R^\mathrm{n}_\mathrm{b}(\mathbf{v}' \to \mathbf{v}) f_{\mathrm{n},\nu-,\mathrm{b}}(\mathbf{v}')) \mathrm{d}\mathbf{v}' & \text{if} \quad \mathbf{v}\cdot\boldsymbol{\nu} > 0, \end{cases} \tag{16}$$

with $\boldsymbol{\nu}$ the inward pointing normal. $f_{\mathrm{i},\nu-,\mathrm{b}}(\mathbf{v})$ and $f_{\mathrm{n},\nu-,\mathrm{b}}(\mathbf{v})$ are respectively the distributions of the incident ions and the incident neutrals. Based on sheath theory, we approximate the incident ion distribution as a half-sided Maxwellian which is possibly accelerated by the sheath potential (if the magnetic field lines are not parallel to the boundary). However, the incident neutral distribution is unknown and the diffusion approach is used to estimate the distribution:

$$f_{\mathrm{n},\nu-}(v_\phi, v_\tau, v_\nu) = \frac{n_\mathrm{i} K_\mathrm{cx,m}}{n_\mathrm{i} K_\mathrm{cx,m} + n_\mathrm{e} K_\mathrm{i}} \widetilde{f}_\mathrm{i}(v_\phi, v_\tau, v_\nu) \left(n_\mathrm{n} - \frac{1}{n_\mathrm{i} K_\mathrm{cx,m} + n_\mathrm{e} K_\mathrm{i}} \left(v_\tau \frac{\partial n_\mathrm{n}}{\partial \tau} + v_\nu \frac{\partial n_\mathrm{n}}{\partial \nu} \right) \right). \tag{17}$$

The distribution is expressed in the (ϕ, τ, ν) coordinate system, with ϕ the toroidal direction, ν the inward pointing normal direction and τ the tangential direction perpendicular to ϕ. v_ϕ, v_τ and v_ν are the particle velocity components in this coordinate system. A detailed derivation of Eq. (17) can be found in Ref. [14]. It should be noted that the simplified Boltzmann equation (Eq. (14)) is used to obtain Eq. (17).

$R^\mathrm{i}_\mathrm{b}(\mathbf{v}' \to \mathbf{v})$ and $R^\mathrm{n}_\mathrm{b}(\mathbf{v}' \to \mathbf{v})$ are the probabilities that an ion or neutral with velocity $\mathbf{v}'$ is recycled or reflected and gets a velocity $\mathbf{v}$. In this paper, we make use of a simplified reflection model. Half of the incident particles are recycled or reflected as fast neutrals, which get half of the energy of the incident particle. The other half of the neutrals are emitted as

molecules (D_2), which are assumed to dissociate immediately by the Franck-Condon process. All neutrals (fast and dissociated) are emitted isotropically.

The particle flux density $\mathbf{\Gamma}^{\mathrm{n}}_{\mathrm{b}}$, the parallel momentum flux density $\mathbf{\Gamma}^{\mathrm{n}}_{\mathrm{m},||,\mathrm{b}}$ and energy flux density $\mathbf{Q}^{\mathrm{n}}_{\mathrm{b}}$ follow from the moments of Eq. (16):

$$\left[\mathbf{\Gamma}^{\mathrm{n}}_{\mathrm{b}} \quad \mathbf{\Gamma}^{\mathrm{n}}_{\mathrm{m},||,\mathrm{b}} \quad \mathbf{Q}^{\mathrm{n}}_{\mathrm{b}}\right] = \int \left[1 \quad mv_{||} \quad \tfrac{m}{2}||\mathbf{v}||^2\right] \mathbf{v} f_{\mathrm{n,b}}(\mathbf{v}) \mathrm{d}\mathbf{v}, \tag{18}$$

and are imposed as boundary fluxes for the corresponding equations, with $v_{||}$ the parallel component of the particle velocity.

5. Results

5.1. Description of the test case

We compare the fluid neutral models with an MC solution of the kinetic equation for a fixed background plasma. This background plasma is extracted from a SOLPS simulation for a typical ITER relevant (partially) detached case with an F12 geometry [15]. We only simulate the outer divertor leg as shown in Fig. 2.

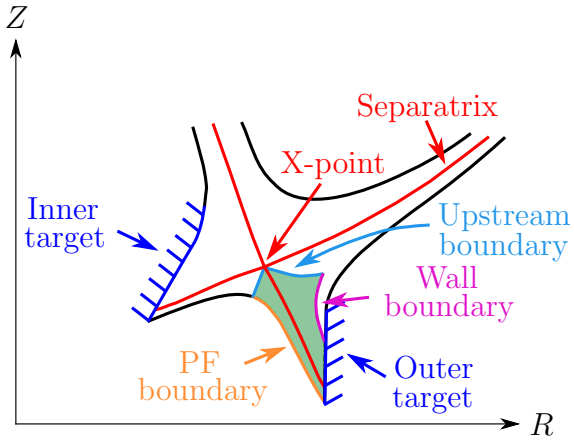

Figure 2: Location of the simulation domain (green shaded area).

In next subsections the plasma sources due to interactions with the neutrals are compared for the different fluid neutral models. These source terms are only significant in a thin region near the target plate. Therefore, only this region is shown in the figures below.

We compare the plasma sources, which are the opposite of the neutral sources given by Eqs. (8)-(10), i.e., $S_{n_{\mathrm{i}}} = -S_{n_{\mathrm{n}}}$, $S_{mu_{||}} = -[\mathbf{S}_m \mathbf{v}_{\mathrm{n}}]_{||}$ and $S_{E,\mathrm{i}} = -S_{E,\mathrm{n}}$. The kinetic solution is based on an MC evaluation of the CX momentum and energy source (Eq. (11)), while the approximate expressions with the momentum linearized rate coefficient are used for all fluid models (Eq. (12) for the momentum and Eq. (15) for the energy source).

5.2. Sources from the MC simulation

Fig. 3 shows the sources from the MC simulation of the exact Boltzmann equation (Eq. (1)). The peak magnitude of the sources is located at the target plate. To make a quantitative assessment of the different models, we will compare the sources in the flux tubes indicated with colors. The global shape of the sources is similar for all models. The peak particle source is located in the blue flux tube, the ion density peaks in the green flux tube and the momentum and ion energy source peak in the red tube. Due to the high temperature the ionization is dominant in the blue flux tube, whereas the low temperature in the red tube gives rise to a high number of CX collisions, which leads to the maximum magnitude of the momentum and ion energy source.

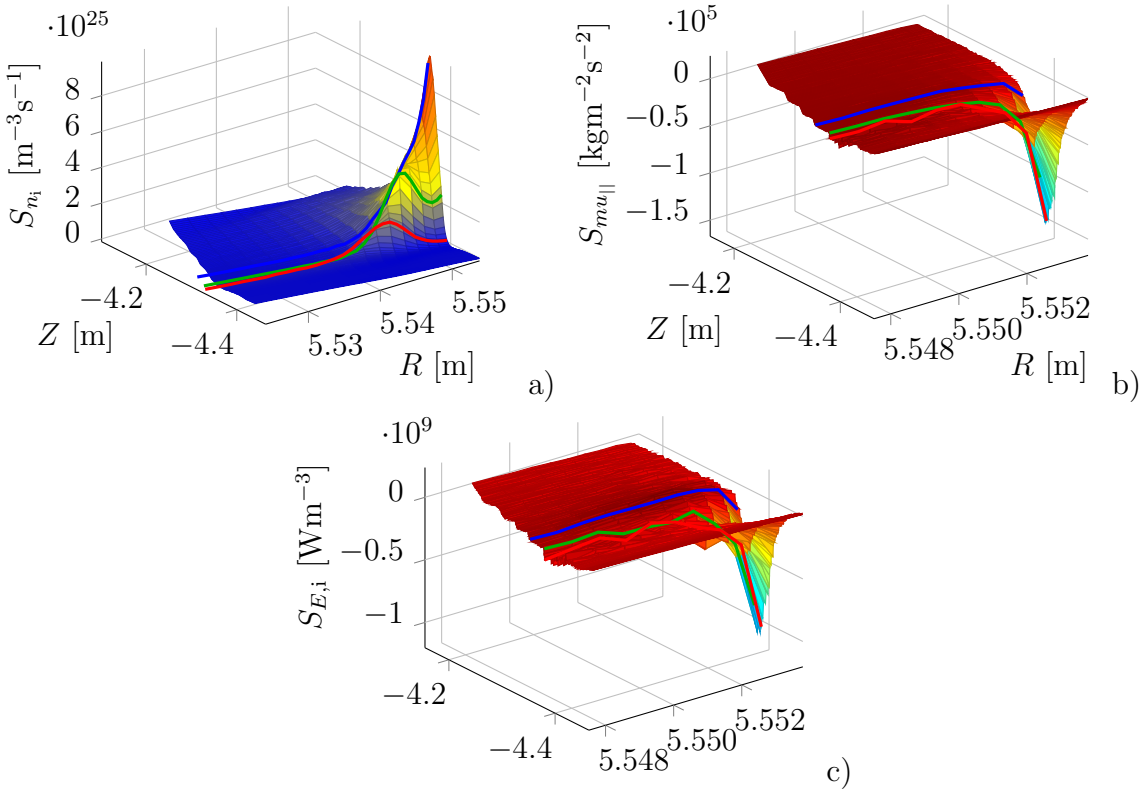

Figure 3: Sources from the MC simulation of the exact Boltzmann equation (Eq. (1)). The red, green and blue lines indicate the sources in the flux tubes which are used for the comparison in next subsections. a) Particle, b) parallel momentum and c) ion energy source.

5.3. Verification of the simplified Boltzmann equation

First, we check the accuracy of the approximate Boltzmann equation (Eq. (14)), which makes use of the momentum linearized CX rate coefficient $K_{\mathrm{cx,m}}$, by comparing the results of the source terms with the solution of the exact Boltzmann equation (Eq. (1)). As can be seen in Fig. 1b, $K_{\mathrm{cx,m}}$ is a function of the average ion-neutral temperature. However, the neutral temperature resulting from an MC simulation is very susceptible to noise and

therefore, we assume $T_\mathrm{n} = T_\mathrm{i}$ for the evaluation of $K_\mathrm{cx,m}$. This approximation is valid for sufficiently small ion-neutral temperature deviations. Fig. 4 shows the results. θ_t is the poloidal distance from the target. It is clear that the simplification has only a minor influence on the results in the region with large sources. In Ref. [16] a detailed derivation is made for the so-called thermal force and diffusion thermoeffect resulting from the velocity dependence of the CX rate coefficient. However, for this CX dominated case the velocity dependence can be neglected if the momentum linearized rate coefficient is taken. This leads to a momentum source that is linear with respect to the ion-neutral velocity difference. This justifies the use of the pressure-diffusion equation (Eq. (13)).

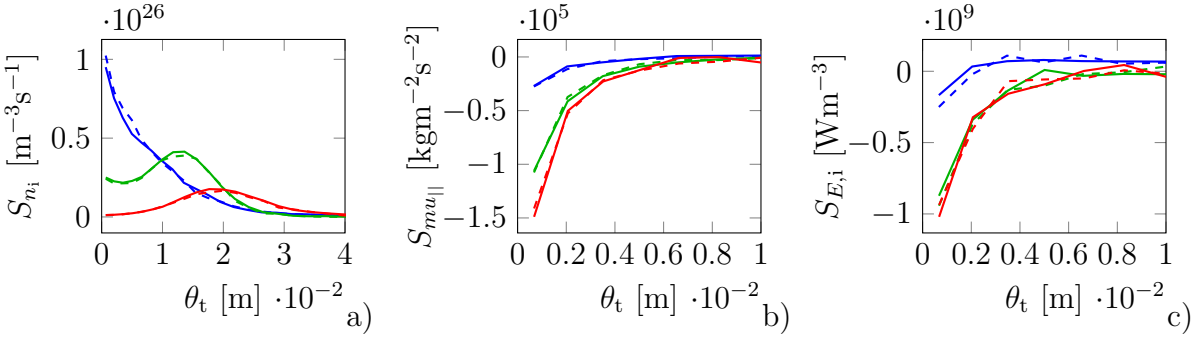

Figure 4: Sources from the exact Boltzmann equation (Eq. (1)) (solid lines) and simplified Boltzmann equation (Eq. (14)) (dashed lines). a) Particle, b) momentum and c) ion energy source.

5.4. Comparison of fluid models

The sources from the different fluid models are compared to the MC solution in Fig. 5.

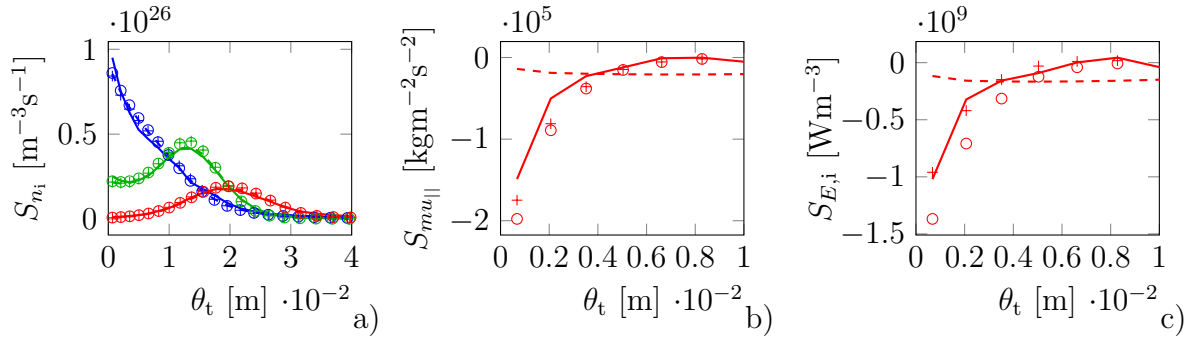

Figure 5: Comparison of sources from fluid models with the MC solution: MC (solid line), pressure-diffusion equation (model 1) (dashed line), pressure-diffusion and parallel momentum equation (model 2) (circles) and pressure-diffusion, parallel momentum and energy equation (model 3) (pluses). a) Particle, b) momentum and c) ion energy source.

All fluid models provide accurate predictions of the particle source with a maximum relative error of about 8% in the cell adjacent to the target of the blue flux tube. The relative differences between the fluid and kinetic models remain smaller than 1% further away from the target. So, even the simple pressure-diffusion model (model 1) can be used

to predict the particle source. The decreased number of CX collisions due to the high temperature in the blue flux tube leads to a decreased validity of the fluid approach (larger deviation from the equilibrium (Maxwellian) distribution).

To not overload the figures, Figs. 5b-c show only the red flux tube where the peak momentum and energy source magnitudes are located. The pure pressure-diffusion equation is totally inaccurate for these sources. At least a parallel momentum equation has to be added to capture the ion-neutral parallel velocity difference in the vicinity of the target. The results are further improved by adding an energy equation. The results for the momentum and ion energy source are extremely sensitive to the boundary condition at the target plate. The new boundary condition from Section 4 performs very well without the use of any fitting parameter.

6. Conclusions

In this paper, we have derived a number of fluid neutral models, fully consistent with the underlying kinetic transport equation. The pressure-diffusion model is a simple model that gives accurate predictions of the particle source (maximum error of about 8%), but fails in (even qualitatively) predicting the momentum and ion energy sources. To obtain qualitatively correct predictions of these sources a parallel momentum equation has to be added with boundary conditions incorporating the underlying physics of the recycling and reflection of the neutrals used in the kinetic description. This is accomplished by imposing boundary fluxes (particle, momentum,...), which result from an estimate of the total neutral velocity distribution at this particular boundary. The diffusion approximation is used for the distribution of the incident neutrals. The parallel momentum in combination with the pressure-diffusion equation gives a slight overestimate of the peak momentum and ion energy source at the target (relative errors of respectively 24 and 27%). This overestimate is reduced by adding a separate neutral energy equation (relative errors of respectively 14 and 1%).

We have shown that it is justified to simplify the CX source/sink term in the Boltzmann equation for this detached case. Although the CX rate coefficient depends on the neutral particle velocity, the use of the so-called momentum linearized CX rate coefficient, which is independent of the particle velocity, gives almost the same results. This is mainly due to the fact that the neutrals obtain the Maxwellian equilibrium distribution already a few mean free paths away from the target. This simplifies the derivation of the fluid models.

The model with the parallel momentum equation is a good starting point for the hybrid model, because it gives already accurate results for all sources. This means that the MC part in the hybrid model can be reduced significantly. The MC part can be further reduced by adding an energy equation, but this leads to an additional cost of the fluid model for solving an extra equation. It has to be investigated whether it is worth the effort.

In future research it is planned to study the coupling of the neutral models with the plasma equations. Given the accuracy of the present results for the source terms, we expect also these simulations to perform well. Nevertheless, it is important to assess the influence of the slight deviations of the fluid from the kinetic solution on the results for the plasma

state. Further, additional physics such as molecules and neutral self-collisions have to be added to the neutral models.

Acknowledgements

This work has been carried out within the framework of the EUROfusion Consortium and has received funding from the Euratom research and training programme 2014-2018 under grant agreement No 633053. The views and opinions expressed herein do not necessarily reflect those of the European Commission. The work of N. Horsten is supported by a PhD grant of the Research Foundation Flanders (FWO Vlaanderen).

References

[1] D. Reiter, M. Baelmans, P. Börner, The EIRENE and B2-EIRENE codes, Fusion Science and Technology 47 (2) (2005) 172–186.
[2] D. Knoll, P. McHugh, S. Krasheninnikov, D. Sigmar, Simulation of dense recombining divertor plasmas with a Navier–Stokes neutral transport model, Physics of Plasmas 3 (1) (1996) 293–303.
[3] M. Rensink, L. Lodestro, G. Porter, T. Rognlien, D. Coster, A comparison of neutral gas models for divertor plasmas, Contributions to Plasma Physics 38 (1-2) (1998) 325–330.
[4] J. Riemann, M. Borchardt, R. Schneider, A. Mutzke, T. Rognlien, M. Umansky, Navier-stokes neutral and plasma fluid modelling in 3D, Contributions to Plasma Physics 44 (1-3) (2004) 35–38.
[5] K. Hoshino, M. Toma, A. Hatayama, D. Coster, X. Bonnin, R. Schneider, H. Kawashima, N. Asakura, Y. Suzuki, Benchmarking kinetic and fluid neutral models with drift effects, Contributions to Plasma Physics 48 (1-3) (2008) 136–140.
[6] M. Furubayashi, K. Hoshino, M. Toma, A. Hatayama, D. Coster, R. Schneider, X. Bonnin, H. Kawashima, N. Asakura, Y. Suzuki, Comparison of kinetic and fluid neutral models for attached and detached state, Journal of Nuclear Materials 390 (2009) 295–298.
[7] C. Karney, D. Stotler, B. Braams, Modeling of neutral plasma in a divertor in the fluid-kinetic transition, Contributions to Plasma Physics 38 (1-2) (1998) 319–324.
[8] D. Reiter, The Data File HYDHEL: Atomic and Molecular Data for EIRENE, Tech. rep., FZ Juelich (2002).
[9] D. Reiter, The data file AMJUEL: Additional atomic and molecular data for EIRENE, Tech. rep., FZ Juelich (2000).
[10] N. Horsten, W. Dekeyser, G. Samaey, P. Börner, M. Baelmans, Fluid neutral model for use in hybrid neutral simulations of a detached case, Contributions to Plasma Physics, Accepted for publication.
[11] N. Horsten, W. Dekeyser, G. Samaey, M. Baelmans, Comparison of fluid neutral models for one-dimensional plasma edge modeling with a finite volume solution of the boltzmann equation, Physics of Plasmas (1994-present) 23 (1) (2016) 012510.
[12] D. Reiter, The EIRENE code user manual (2009).
[13] A. Bobylev, The Chapman-Enskog and Grad methods for solving the Boltzmann equation, in: Akademiia Nauk SSSR Doklady, Vol. 262, 1982, pp. 71–75.
[14] N. Horsten, G. Samaey, M. Baelmans, Assessment of fluid neutral models for an ITER relevant detached case, In preparation for Nuclear Fusion.
[15] A. Kukushkin, H. Pacher, V. Kotov, D. Reiter, D. Coster, G. Pacher, Effect of conditions for gas recirculation on divertor operation in ITER, Nuclear fusion 47 (7) (2007) 698.
[16] P. Helander, S. Krasheninnikov, P. Catto, Fluid equations for a partially ionized plasma, Physics of Plasmas (1994-present) 1 (10) (1994) 3174–3180.